JACS
JOURNAL OF THE AMERICAN CHEMICAL SOCIETY
Article
pubs.acs.org/JACS

Deciphering How Pore Formation Causes Strain-Induced Membrane Lysis of Lipid Vesicles

Joshua A. Jackman,[†] Haw Zan Goh,[†] Vladimir P. Zhdanov,[†,§] Wolfgang Knoll,[†,∥] and Nam-Joon Cho*[,†,‡]

[†]School of Materials Science and Engineering and Centre for Biomimetic Sensor Science, Nanyang Technological University, 50 Nanyang Drive 637553, Singapore

[‡]School of Chemical and Biomedical Engineering, Nanyang Technological University, 62 Nanyang Drive 637459, Singapore

[§]Boreskov Institute of Catalysis, Russian Academy of Sciences, Novosibirsk 630090, Russia

[∥] Austrian Institute of Technology (AIT), Donau-City-Strasse 1, 1220 Vienna, Austria

Supporting Information

ABSTRACT: Pore formation by membrane-active antimicrobial peptides is a classic strategy of pathogen inactivation through disruption of membrane biochemical gradients. It remains unknown why some membrane-active peptides also inhibit enveloped viruses, which do not depend on biochemical gradients. Here, we employ a label-free biosensing approach based on simultaneous quartz crystal microbalance-dissipation and ellipsometry measurements in order to investigate how a pore-forming, virucidal peptide destabilizes lipid vesicles in a surface-based experimental configuration. A key advantage of the approach is that it enables direct kinetic measurement of the surface-bound peptide-to-lipid (P:L) ratio. Comprehensive experiments involving different bulk peptide concentrations and biologically relevant membrane compositions support a unified model that membrane lysis occurs at or above a critical P:L ratio, which is at least several-fold greater than the value corresponding to the onset of pore formation. That is consistent with peptide-induced pores causing additional membrane strain that leads to lysis of highly curved membranes. Collectively, the work presents a new model that describes how peptide-induced pores may destabilize lipid membranes through a membrane strain-related lytic process, and this knowledge has important implications for the design and application of membrane-active peptides.

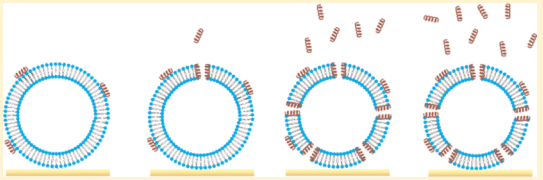

INTRODUCTION

Numerous antiviral strategies have emerged in response to the continued proliferation and rapid evolution of viral pathogens.[1] As obligate parasites, viruses critically depend on host cells to facilitate viral replication and packaging. Antiviral drugs can impair hijacked host cell factors in order to abrogate virion production or stimulate the host immune response.[2] Direct-acting antiviral drugs are becoming more prevalent and inhibit viral proteins involved in viral entry or genome replication.[3] This approach lends strong potential to the development of highly selective therapies, but the effectiveness can be fleeting because escape mutants may quickly arise through error-prone cycles of genome replication. For many viruses, mature virions also possess a lipid bilayer envelope that is important for maintaining virus structure and infectivity.[4] The virion envelope itself is an attractive pharmacological target because its lipid bilayer is derived from the host cell and has an appreciably higher barrier to evolution.

The search for membrane-active antiviral drugs targeting the virion envelope is ongoing, and motivated by the large number of clinically significant enveloped viruses such as HIV and influenza. Compared to other classes of direct-acting antiviral drugs, the mechanisms of action of drugs in this class are more nebulous with details of the molecular interactions still open to investigation. For example, two antiviral agents of this category were originally thought to intercalate into the virion envelope and increase positive membrane curvature,[5,6] while more recent evidence suggests that they are both photosensitizing agents, which cause the hydroxylation of unsaturated phospholipids leading to membrane ordering and reduced fluidity.[7,8] One of the most outstanding questions that remains for antiviral agents in this class concerns pore-forming virucidal peptides which lyse virion envelopes.[9,10] Unlike more well-studied antibacterial peptides, virucidal peptides are not selective on the basis of lipid composition but rather demonstrate membrane curvature sensing in order to distinguish sub-100 nm diameter virion envelopes from appreciably larger cellular membranes.[11,12] Furthermore, while pore formation in bacterial membranes is sufficient to destabilize biochemical gradients, viruses lack biogenic capacity which suggests that pore formation in this context has different, albeit unknown consequences. A key question relates to understanding why pore formation by certain membrane-active peptides can inhibit enveloped viruses.

Herein, we employ a label-free biosensing approach to explore this question by investigating how a pore-forming, virucidal peptide destabilizes lipid vesicles in a surface-based experimental configuration. The lipid vesicles mimic the

Received: December 2, 2015
Published: January 11, 2016

DOI: 10.1021/jacs.5b12491
J. Am. Chem. Soc. 2016, 138, 1406−1413

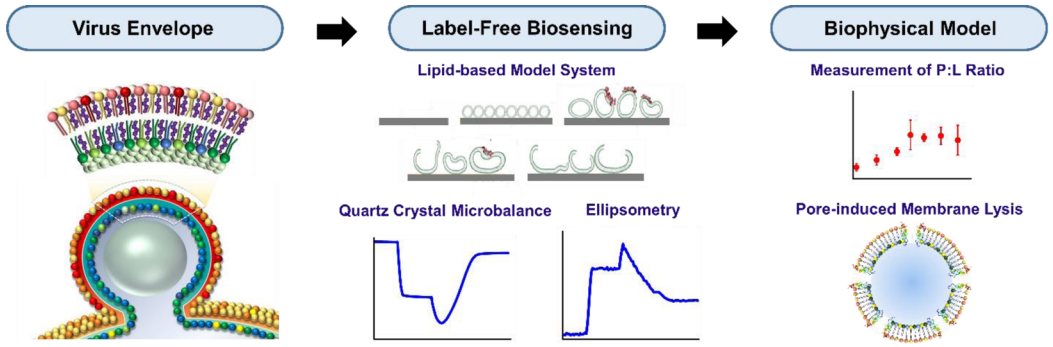

Figure 1. Scheme of experimental strategy to measure the P:L ratio for a virucidal peptide. Membrane-active virucidal peptides interfere with the lipid bilayer surrounding enveloped virus particles. In order to characterize the membrane-peptide interaction, a lipid-based model system comprised of substrate-supported adsorbed vesicles was utilized with simultaneous quartz crystal microbalance-dissipation and ellipsometry measurements. The P:L ratio associated with membrane lysis was directly measured based on the surface-bound lipid and peptide concentrations, which are not possible to measure using conventional experimental methods. With this approach, a new model for pore-induced membrane lysis of highly curved lipid membranes is introduced.

geometrical size of susceptible, sub-100 nm diameter virion envelopes and possess a tunable membrane composition of phospholipids and sterols in order to interrogate how compositional factors influence the membrane-peptide interaction. Importantly, our experimental approach takes advantage of surface-sensitive measurement tools that enable the direct kinetic measurement of the stoichiometric ratio of bound peptides and lipids in the system, a value which has long been difficult to obtain in conventional vesicle assays in bulk solution. In turn, we are able to calculate the bound peptide-to-lipid (P:L) ratio, and interpret our findings using a generic kinetic model in order to explain how the virucidal peptide induces membrane lysis upon forming a critical density of pores in lipid vesicles.

EXPERIMENTAL SECTION

Membrane Reagents. Lipids and sterols were obtained from Avanti Polar Lipids (Alabaster, AL, USA). Lipids, used as-supplied in chloroform, included 1-palmitoyl-2-oleoyl-*sn*-glycero-3-phosphocholine (POPC), 1-palmitoyl-2-oleoyl-*sn*-glycero-3-phospho-L-serine (sodium salt) (POPS), 1-palmitoyl-2-oleoyl-*sn*-glycero-3-phosphoethanolamine (POPE), 1-palmitoyl-2-oleoyl-*sn*-glycero-3-ethylphosphocholine(chloride salt) (POEPC), and sphingomyelin (brain, porcine). Cholesterol (ovine wool, > 98%) was obtained in dry powder form and subsequently solubilized in chloroform with a trace amount of methanol. Lipids and sterols were mixed in organic solvent to the desired molar ratio before vesicle preparation as described below. The molar ratio of the HIV envelope-mimicking composition was chosen as POPC:POPE:POPS:SM:Chol (9.35:19.25:8.25:18.15:45.00).

Vesicle Preparation. Small unilamellar vesicles were obtained by the extrusion method as follows. Lipid films were prepared by first drying lipids in chloroform under a gentle stream of nitrogen air at room temperature. The resulting dry lipid film was then stored under vacuum overnight to remove residual chloroform. Multilamellar vesicles were then generated by swelling the dry lipid film in aqueous buffer solution at a lipid concentration of 5 mg·mL^{-1}, and then the solution was subjected to vortexing. The resulting multilamellar vesicles were extruded by using a Mini Extruder (Avanti Polar Lipids) through a polycarbonate membrane with 50 nm diameter pores and then again through a polycarbonate membrane with 30 nm diameter pores. The only exception was vesicle samples containing 45 mol % Chol. Due to the high cholesterol content which increases membrane bending rigidity, extrusion was performed through 50 nm pores only. Vesicle solutions were diluted before experiment to 0.125 mg·mL^{-1}, and were used within 3 days of preparation. For QCM-D and ellipsometry measurements, an aqueous buffer solution of 200 mM NaCl and 10 mM Tris (pH 7) was used. All buffers and solutions were prepared with 18.2 MΩ·cm Milli-Q-treated water (MilliPore, Oregon, USA).

Peptide. High purity AH peptide (>95%) was synthesized by Anaspec Corporation (San Jose, CA, USA). The sequence of the AH peptide is H-Ser-Gly-Ser-Trp-Leu-Arg-Asp-Val-Trp-Asp-Trp-Ile-Cys-Thr-Val-Leu-Thr-Asp-Phe-Lys-Thr-Trp-Leu-Gln-Ser-Lys-Leu-Asp-Tyr-Lys-Asp-NH_2. The as-supplied lyophilized form was initially solubilized in DMSO and then diluted in water in order to prepare a stock concentration of 2 mg·mL^{-1} peptide (8% DMSO). The exact molar concentration of peptide in solution was determined by standard absorbance measurements at 280 nm.[13] For experiment, the peptide stocks were diluted with aqueous buffer solution [10 mM Tris (pH 7) and 200 mM NaCl] and the final DMSO concentration was less than 0.3%.

Dynamic Light Scattering. The corresponding measurements were performed on a 90Plus Particle Size Analyzer (Brookhaven Instruments Corporation, New York, USA) at a scattering angle of 90° where the reflection effect is minimized. All autocorrelation functions obtained were analyzed by the cumulants method and fitted to a log-normal distribution in order to obtain the vesicle size distribution.

Quartz Crystal Microbalance-Dissipation (QCM-D). The experiments were performed on a Q-Sense E1 instrument (Q-Sense AB, Gothenburg, Sweden). Experimental data were collected at several overtones (n = 3, 5, 7, 9), and the changes in frequency (Δf) and energy dissipation (ΔD) were monitored as a function of time. The reported measurement values are from the third overtone (n = 3) and were normalized accordingly ($\Delta f_{n=3}/3$). All measurements were performed on QCM-D sensor crystals (Q-Sense AB) with titanium oxide coats. The substrates were cleaned with 1% w/w sodium dodecyl sulfate (SDS) solution, and then rinsed with water and ethanol, sequentially. After gentle drying with a stream of nitrogen air, the crystals were subjected to oxygen plasma treatment (Harrick Plasma, Ithaca, NY, USA) for ∼1 min immediately before experiment.

Ellipsometry. A Nanofilm EP3 ellipsometer (Accurion GmbH, Germany) with the EP3View software package was used for simultaneous optical measurement on the same substrate as for the QCM-D measurements. For this purpose, a QCM-D measurement chamber (QELM 401, Q-Sense AB) was employed, which has two optical windows to permit ellipsometric measurement at incident and reflected angles of 65°. The incident light had a wavelength of 545.6 nm which was selected from a xenon lamp by using an interference filter. The measured Δ and Ψ signals were fit to a layered structure in order to determine the complex refractive index and thickness of each layer by using the EP4Model software (Accurion GmbH). To obtain the optical properties of the substrates, measurements were conducted in water (n = 1.333), buffer (n = 1.335), and isopropanol (n = 1.378). Lipid layers deposited on the substrate were modeled as a homogeneous adlayer with a refractive index n and a thickness d. n

DOI: 10.1021/jacs.5b12491
J. Am. Chem. Soc. 2016, 138, 1406−1413

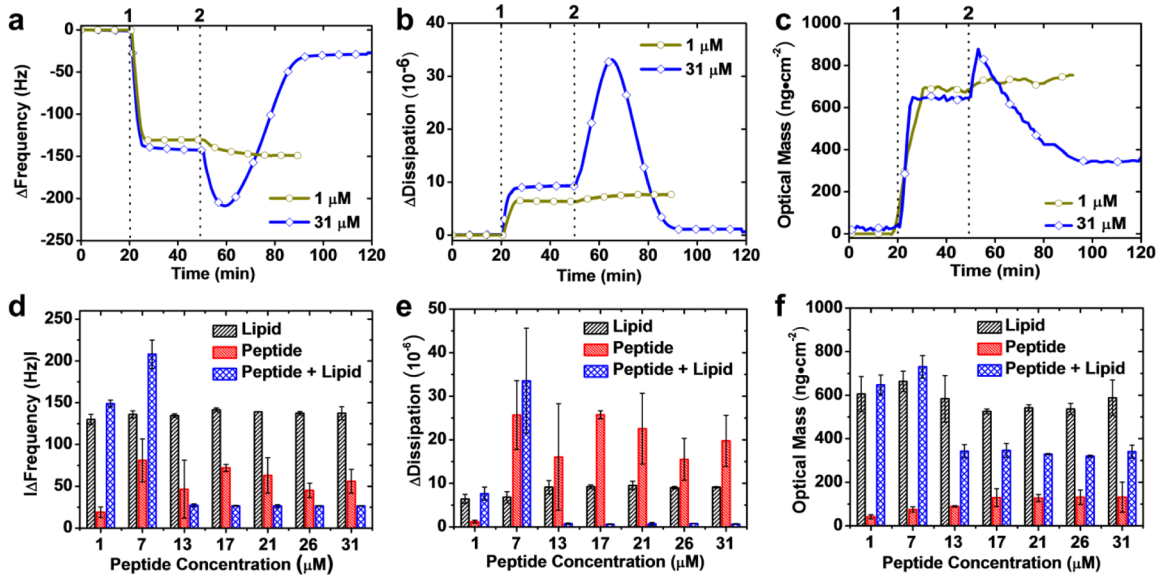

Figure 2. Rupture of POPC lipid vesicles by AH peptide. (a,b) Representative QCM-D frequency and energy dissipation shifts observed during interaction of AH peptide with surface-adsorbed vesicles at different peptide concentrations in solution. Labels 1 and 2 indicate vesicle and peptide addition, respectively. (c) Optical mass shifts obtained by simultaneous ellipsometric monitoring of the same process. (d–f) Summary values of QCM-D and ellipsometry shifts for peptide-induced vesicle rupture at different peptide concentrations. "Lipid" refers to the adsorbed vesicle layer, "peptide" refers to the additional adsorbed peptide, and "peptide + lipid" refers to the final layer after the rupture process is complete. Each point is the average of three measurements with the corresponding standard deviation.

was constrained from 1.33 (refractive index of water) to 1.5 (refractive index of a lipid bilayer), and d was constrained from 0 to 100 nm. The optical mass of the layer, $\Delta m_{optical}$, was determined from n_{layer} and d_{layer} by using the de Feijter formula.

RESULTS

Measurement of Peptide Surface Concentration. The membrane activity of peptides is typically characterized by monitoring the release of entrapped markers from vesicles in bulk solution.[14] With a given number of vesicles in solution, the lowest peptide concentration that induces marker release is defined as a critical value based on the ratio of the peptide and lipid bulk concentrations. On a comparative scale, these values are well-established for assessing the surface activity of a peptide.[15,16] However, there is only weak correlation between these values and anti-infective activity in biological systems.[17,18] One issue concerns the limited quantification afforded by conventional solution-based measurements. In bulk vesicle experiments, the fraction of bound peptide at attachment-detachment equilibrium can vary significantly (typically between 10% and 100% of total peptide in solution[19]), and the stoichiometric fraction of bound peptide during different stages of the membrane-peptide interaction is unknown. In order to measure the peptide surface concentration, alternative experimental strategies are needed.

To address this issue, we have employed a surface-sensitive measurement approach that includes a layer of adsorbed lipid vesicles on a titanium oxide surface (Figure 1). Vesicles with controlled membrane composition and size are prepared by the extrusion method, and then deposited on the substrate. The vesicles adsorb and form a close-packed layer. Then, the membrane-active amphipathic, α-helical (AH) peptide with known broad-spectrum virucidal activity[10] is added to induce vesicle destabilization and membrane lysis.[20] The entire process is monitored in real-time without label by simultaneous QCM-D[21] and ellipsometry[22] measurements that can follow different stages in the AH peptide-membrane interaction. The interaction results in changes in physical properties of the adsorbed vesicle layer, which are directly tracked by the two measurement techniques.[23] The QCM-D technique is an acoustic sensor technique that measures the resonance frequency and energy dissipation of an oscillating titanium oxide-coated quartz crystal. When an adsorbate attaches to the titanium oxide-coated sensor surface, there are shifts in the frequency (Δf) and energy dissipation (ΔD) of the quartz crystal, which can be tracked as a function of time and correspond to the acoustic mass and viscoelastic properties of the adsorbate, respectively. Simultaneously, the ellipsometry technique measures changes in effective film polarization, which can be converted to the optical mass of the adsorbate. The QCM-D acoustic mass accounts for the wet mass (e.g., lipid, peptide and coupled solvent), and the ellipsometric optical mass reflects the dry mass of the adsorbate (e.g., lipid and peptide only). Taking advantage of these simultaneous measurements, we utilized the ellipsometric measurement readout to record the mass of added lipids and peptide at each step, and followed the kinetics of the vesicle destabilization process with the QCM-D measurement signals. This combined approach therefore allowed us to measure the surface-bound peptide concentration, and corresponding P:L ratio, at different stages of the vesicle destabilization process.

Determination of Threshold Peptide Concentration. We first examined the interaction between AH peptide and surface-adsorbed vesicles composed of POPC lipid (Figure 2a–c). Extruded vesicles (less than 60 nm diameter; Table S1) were deposited on a titanium oxide substrate almost up to saturation. The corresponding QCM-D adsorption kinetics are consistent with formation of a close-packed, adsorbed vesicle layer ($\Delta f \approx -130$ Hz and $\Delta D \approx 7 \times 10^{-6}$). The optical mass of the adsorbed vesicle layer was 590 ± 87 ng·cm^{-2}. AH peptide was then added and, depending on its concentration in solution, resulted in peptide binding without or with

DOI: 10.1021/jacs.5b12491
J. Am. Chem. Soc. 2016, 138, 1406–1413

subsequent vesicle rupture as explained below. The extent of vesicle rupture was interpreted by the structural transformation of the adsorbed vesicle layer into a supported lipid bilayer, which signifies the rupture of all surface-bound vesicles.[10] At low peptide concentration (e.g., 1 μM peptide treatment), peptide attachment led to additional frequency and energy dissipation shifts and corresponding uptake in the total optical mass due to bound peptide. In this case, there was no vesicle rupture. By contrast, at high peptide concentration (e.g., 31 μM peptide treatment), a rapid decrease in Δf and ΔD was initially observed due to peptide attachment followed by positive shifts and a corresponding drop in the optical mass which are associated with vesicle rupture.

A summary of the acoustic and optical measurement responses demonstrates a strong dependence of vesicle rupture on the bulk peptide concentration (Figure 2d–f). In the low concentration regime (below 13 μM), AH peptide binding caused incomplete rupture. At 1 μM peptide concentration, monotonic peptide adsorption was observed (final Δf and $\Delta D \approx -150$ Hz and 7×10^{-6}, respectively). Although the amount of bound peptide was appreciable ($\Delta f \approx -20$ Hz), it is likely that membrane destabilization was insignificant because there was only a minor change in the viscoelastic properties of the adsorbed vesicle layer. The corresponding optical mass shift due to peptide adsorption was around 42 ng·cm^{-2}. By contrast, at 7 μM peptide concentration, more appreciable membrane destabilization occurred, as indicated by larger changes in frequency and energy dissipation that are indicative of strain-related membrane protrusions and related structural deformations.[24,25] However, the destabilization process in this case did not lead to complete vesicle rupture based on the final measurement responses. The optical mass shift was around 75 ng·cm^{-2}, which supports that the amount of bound peptide increased at higher bulk peptide concentrations.

In the high peptide concentration regime (at or above 13 μM), complete vesicle rupture was observed. Initially, AH peptide binding caused an increase in adsorbed mass that led to maximum changes in frequency and energy dissipation of approximately -210 Hz and 30×10^{-6}, respectively. After reaching the maximum change in frequency, vesicle rupture occurred due to membrane lysis and resulted in the formation of a supported lipid bilayer, as indicated by final $\Delta f \approx -26$ Hz and $\Delta D < 0.5 \times 10^{-6}$. The change in film properties (interpreted by the $\Delta f/\Delta D$ ratio[26]) that was caused by the AH peptide-mediated structural transformation occurred largely independent of the peptide concentration in solution (Figure S1). Furthermore, in this high peptide concentration regime (especially 17 μM AH peptide and higher), the maximum change in optical mass was consistently around 130 ± 50 ng·cm^{-2}, which indicates that a critical amount of bound peptide is required for vesicle rupture. Hence, the data indicate that, above a certain bulk peptide concentration, bound AH peptide reaches a critical mass density on the vesicle surface, which induces membrane lysis, and in turn vesicle rupture. On the other hand, vesicle rupture is not observed at lower mass densities. In order to understand the physical basis for peptide-induced membrane lysis at or above the critical peptide density, we next consider the known pore-forming behavior of AH peptide in highly curved membranes such as those found in the lipid vesicles under consideration.

Membrane Lysis Depends on the Number of Pores. In order to understand how the pore-forming AH peptide induces membrane lysis, we analyzed the vesicle rupture time, t_r, associated with the aforementioned experiments. Vesicle rupture is a stochastic process and accordingly the rupture-time distribution of individual vesicles may be relatively broad even if the vesicle size is fixed. In our approach, the rupture time was defined as the period from initial peptide attachment until there was rupture of most adsorbed vesicles ($\Delta f > -45$ Hz, as compared to the baseline; see also Figure S2). This time was found to be inversely proportional to peptide concentration, c, in solution,

$$t_r \propto 1/c^{\beta} \quad (1)$$

where $\beta = 0.97 \pm 0.20$ (Figure 3). We also calculated the P:L ratio corresponding to vesicle rupture based on the optical

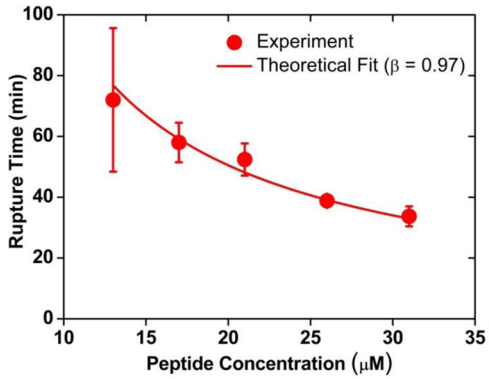

Figure 3. Rupture time of supported lipid vesicles as a function of AH peptide concentration in solution. Fit was obtained by $Ac^{-\beta}$, where A and β are fitting parameters. Each point is the average of three measurements with the corresponding standard deviation.

masses of lipid (L) in the adsorbed vesicle layer and the maximum amount of bound peptide (P). Under conditions when vesicle rupture occurred, the P:L ratio was approximately 1/25 (Figure 4). If the P:L ratio was lower, then complete vesicle rupture did not occur. Of note, the P:L ratio in all cases was significantly higher than the critical P:L ratio for the onset of pore formation, which has been estimated to be between 1/100[27] and 1/1000[11] for the AH peptide under consideration. Hence, the measurements indicate that there is an appreciable stoichiometric difference in the P:L ratio required for AH

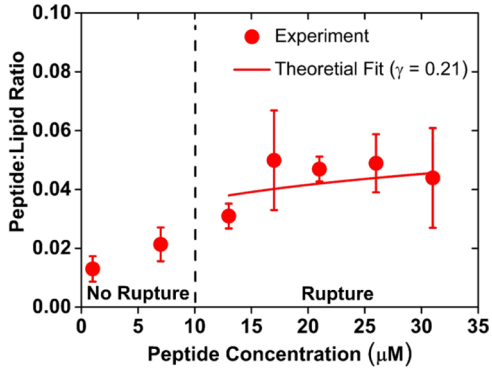

Figure 4. Equilibrium P:L ratio for AH peptide-mediated vesicle rupture. L and P are the optical mass of the adsorbed vesicle layer and maximum bound peptide, respectively. Fit in the vesicle rupture regime was obtained by Ac^{γ}, where A and γ are fitting parameters. Each point is the average of three measurements with the corresponding standard deviation.

DOI: 10.1021/jacs.5b12491
J. Am. Chem. Soc. 2016, 138, 1406–1413

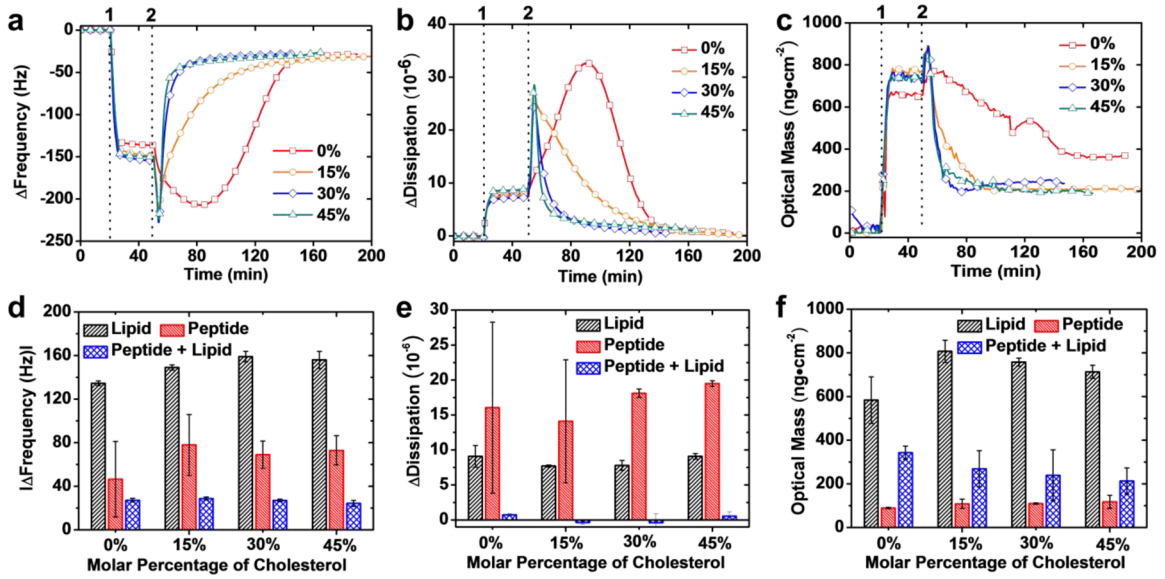

Figure 5. Dependence of peptide-induced vesicle rupture on cholesterol fraction. (a,b) Representative Δf and ΔD shifts for peptide-induced vesicle rupture at varying cholesterol fractions (mol %) in lipid vesicles. Labels 1 and 2 indicate the time of vesicle and peptide addition, respectively. (c) Optical mass shifts for the same process. (d–f) Summary values of Δf, ΔD, and optical mass shifts. All data were collected at 13 μM peptide concentration. Each point is the average of three measurements with the corresponding standard deviation.

peptide-mediated membrane permeabilization versus lysis, the latter of which requires a critical number of pores and is likely relevant in the context of virucidal activity against the lipid membranes surrounding enveloped viruses which do not depend on biochemical gradients.

Physically, vesicle rupture occurs via peptide-induced pore formation in and structural rearrangement of the vesicle's lipid bilayer.[11,24] In turn, pore formation is limited by peptide nucleation.[28] The dependence of the rate of the latter process on the number, N, of peptides attached to a vesicle is expected to be highly nonlinear, which appears initially to contradict $\beta \approx 1$. To illustrate that $\beta \approx 1$ is in fact consistent with the nucleation concept, we note that the dependence of N on time depends on the adsorption conditions. If adsorption is controlled by diffusion under flow conditions, one is expected to have $N \propto ct$. Under kinetically controlled conditions, the dependence of N on t can often be approximately described by the conventional power-law equation, $N \propto (ct)^{\alpha}$, where $\alpha < 1$ or > 1 for competitive or cooperative adsorption, respectively. Our previous study[24] determined that α is 1.4, i.e., the adsorption is cooperative. Focusing on this case and identifying N with the number of monomers, we can use the simplest expression for the nucleation rate, $W \propto N^n \propto (ct)^{\alpha n}$, where n is the nucleation order independent of N (this is the case if the process involves only a few peptides, i.e., n is small; in addition, pore formation is considered to occur primarily above its corresponding P:L ratio, and this ratio is not introduced explicitly). Although this phenomenological expression for W does not describe explicitly all the details of pore formation, it is sufficient in order to relate the rates of adsorption and pore formation. Its use implies that the surface peptide concentration is above the critical one for pore formation. In other words, it implies that ct is not too low. For the initial stage of the kinetics where ct is low, the power-law expression for W predicts a negligible rate of pore formation. For this reason, we can integrate W from 0 to t in order to obtain the number of pores, N_p, which is accordingly given by

$$N_p = \int_0^t W(t')\,dt' \propto c^{\alpha n} t^{\alpha n+1} \tag{2}$$

The simplest physically reasonable condition for vesicle rupture is to consider that it happens in a stepwise fashion (as in percolation-type processes) or more gradually (with membrane solubilization) when N_p reaches the critical value. In combination with eq 2, this condition yields $\beta = \alpha n/(\alpha n + 1)$. Employing $n = 4$ and $\alpha = 1.4$ based on our previous works,[11,24] we obtain $\beta = 0.9$, which is in agreement with the present observation. Thus, this generic analysis explains why β may be close to 1 despite the complexity of the degradation process, and also why the peptide uptake at the onset of rupture, $N \propto (ct_r)^{\alpha} \propto c^{\alpha/(\alpha n+1)}$, is nearly independent of c (provided $\alpha \approx 1$ and $n \geq 4$).

Cholesterol Restricts Membrane Deformation. To understand how biological factors influence the membranolytic behavior of AH peptide, we next investigated the interaction between AH peptide and cholesterol-enriched lipid vesicles (Figure 5). An abundant component of human cell membranes, cholesterol is found in large quantities in the membrane surrounding enveloped viruses.[29] The effects of cholesterol on lipid membranes are diverse.[30] It facilitates lateral excess to lipid headgroups and increases membrane bending rigidity (especially in the case of saturated lipids), and decreases membrane permeability by small molecules. Across a wide range of cholesterol fractions (0–45 mol %), it was identified that 13 μM AH peptide induces vesicle rupture. Interestingly, the experimentally measured rupture kinetics were appreciably shorter for cholesterol-enriched vesicles (Figure 5a–c). While cholesterol increases the bending rigidity of lipid vesicles, this stabilization comes at the expense of vesicle deformability leading to more abrupt rupture. Importantly, independent of the cholesterol fraction, peptide-induced membrane lysis followed a similar process as the critical P:L ratio remained approximately 1/25, further supporting that pore formation is the principal cause of vesicle degradation (Figure 5d–f).

DOI: 10.1021/jacs.5b12491
J. Am. Chem. Soc. 2016, 138, 1406–1413

To further investigate how the critical P:L ratio depends on the membrane composition, we performed additional experiments on lipid-cholesterol vesicles over a wide range of peptide concentrations (Figure 6). Experiments were also performed on

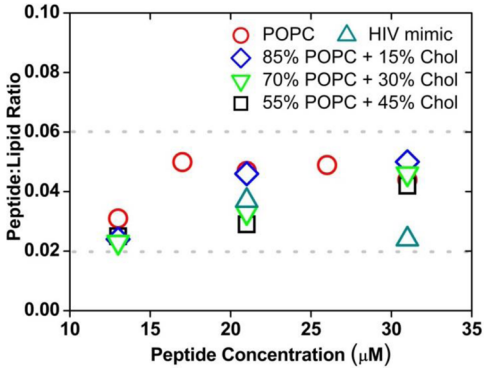

Figure 6. Peptide-to-lipid ratio of peptide-induced vesicle rupture for varying lipid compositions. The P:L ratio is plotted based on the optical mass corresponding to the intact vesicle adlayer (L) and maximum amount of bound peptide (P) in each individual experiment. The dashed lines illustrate that the critical P:L ratio was between approximately 1/50 and 1/20 for all membrane compositions. Each point is the average of three measurements.

HIV envelope-mimicking vesicles containing several kinds of phospholipids (POPC, POPE, and POPS), sphingomyelin, and a high fraction of cholesterol (Figures S3–S6). Interestingly, the critical P:L ratio for vesicle degradation remained consistently around 1/25 with a weak dependence on peptide concentration as noted above. Compared to the zwitterionic lipid composition, the degradation of HIV envelope-mimicking vesicles was appreciably quicker. Negatively charged lipids are known to increase the rate of vesicle degradation and may play a role in this case.[31] Surprisingly, despite the wide range of lipid compositions employed in this study, a general trend in P:L ratio corresponding to vesicle degradation was observed. This finding leads us to conclude that membrane lysis by AH peptide requires a critical number of peptide-induced pores largely independent of membrane composition.

DISCUSSION

Membrane-active peptides have long attracted interest as antimicrobial compounds. A classic example is antibacterial peptides, which destabilize bacterial cell membranes. Such peptides are typically cationic and prefer negatively charged lipid compositions in model systems.[32] The prevailing model[33,34] describing the molecular mechanism of peptide-induced pore formation in lipid bilayers is gleaned from equilibrium and kinetic studies involving antibacterial peptides. The model takes into account the surface concentration of peptides oriented along the membrane (S state) and inserted into the membrane in perpendicular direction (I state). The S–I transition is believed to be related to the membrane strain induced by peptides in the S state and to exhibit a sigmoidal dependence on peptide concentration that is typically characterized by a critical value in the molar ratio of bound peptide (P) to lipid (L) molecules in the system.[35,36] Above this critical ratio, a phase transition occurs via peptide nucleation that leads to the formation of stable pores and an increase in the effective bending modulus of the membrane.[37,38] So far, extension of this model to the mechanism of action of virucidal peptides has been lacking for several reasons.

First, virucidal peptides preferentially target highly curved lipid membranes such as small vesicles and viral envelopes. Membrane curvature imposes membrane strain, and these vesicular structures are prone to pore formation and rupture. In contrast to antibacterial peptides, the rate of pore formation of virucidal peptides increases with decreasing vesicle size and this step is facilitated by the membrane strain.[28] Coincident with pore formation, it has been experimentally observed that supported vesicles undergo membrane alterations that may be considered as a response to the changing energy landscape arising from the pores along with unbalanced peptide adsorption on the outer lipid leaflet. We may note that these previous observations are restricted to fluid-phase lipid compositions and our current experiments with lipid-cholesterol vesicles have led to a more complete picture of how virucidal peptides act against biologically relevant membrane compositions. In particular, curved membranes with significant cholesterol fractions have appreciably higher bending rigidities and are less deformable. In such case,

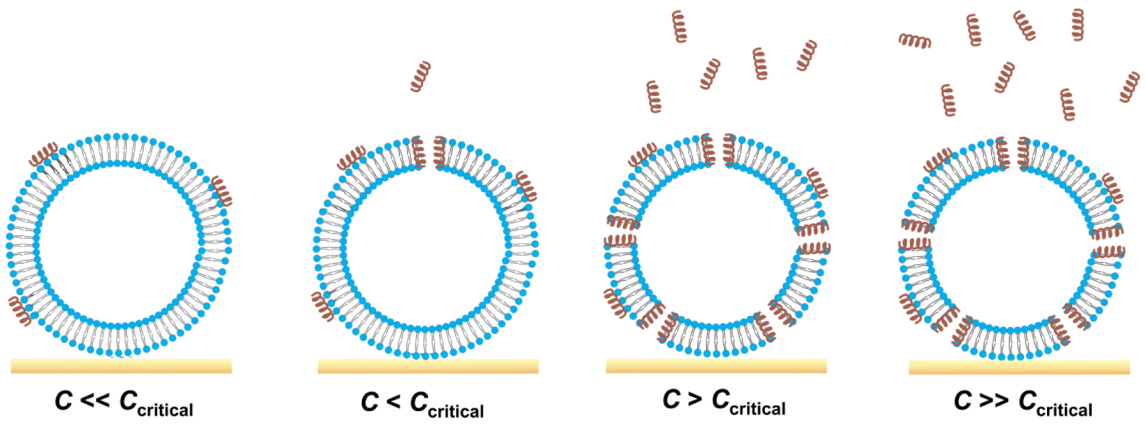

Figure 7. Physical model of membrane lysis at the critical pore concentration. At very low peptide concentrations (c), there is a proportional increase in the amount of bound peptide monomers. Above a certain peptide concentration, peptide monomers assemble into pores in the lipid membrane. The number of pores in the membrane increases with increasing peptide bulk concentration. Above a critical peptide concentration ($c_{critical}$), the number of pores in the membrane reaches a sufficiently high density in order to induce membrane lysis. Vesicle rupture occurs only at or above $c_{critical}$.

DOI: 10.1021/jacs.5b12491
J. Am. Chem. Soc. 2016, 138, 1406–1413

peptide-induced pore formation likely increases the bending modulus of the membrane until the additional stress can no longer be accommodated leading to disintegrative membrane lysis.

A related issue concerns the experimental measurement of the surface concentration of attached peptides. Despite its perceived importance in theoretical models, this value cannot be measured by conventional experimental techniques. With our measurement approach, we were able to determine the P:L ratio over a wide range of peptide concentrations and membrane compositions. Importantly, the findings support that there is a nearly constant P:L ratio associated with membrane lysis, which can be explained by a critical number of pores in the membrane, i.e., a critical pore concentration (Figure 7). By tracking the surface-bond peptide mass, we deduced that a critical number of pores is required for membrane lysis. How a critical number of pores induces lysis of a highly curved membrane such as a sub-100 nm diameter lipid vesicle is an intriguing question. As mentioned above, the physics of peptide-induced pore formation supports that there is an increase in the bending modulus, which induces membrane destabilization. At a certain energy threshold, the vesicular structure fails due to the combination of membrane curvature-related and pore-related stress in the membrane. These factors appear to be more influential than membrane composition, although the latter may strongly affect the rate of pore formation. While the destabilization process is caused by peptide-induced pores, the resulting process of membrane lysis likely involves membrane solubilization arising from the interaction between amphipathic peptides and lipids.[39,40] Hence, the virucidal AH peptide takes advantage of the membrane strain in highly curved membranes in order to form pores while simultaneously further destabilizing the membrane and inducing membrane lysis.

CONCLUSIONS

In summary, we have employed a combination of surface-sensitive measurement techniques in order to track the bound peptide mass during the interaction between the virucidal AH peptide and supported lipid vesicles. This experimental approach allowed us to calculate the surface-bound P:L ratio, which is an important value to describe the surface activity of membrane-active peptides. In particular, we were able to identify that membrane lysis occurs at a critical P:L ratio that is well above the P:L ratio corresponding to the onset of pore formation for AH peptide, offering a new mechanistic model to describe the membrane-lytic behavior of this virucidal peptide. The findings indicate that peptide-induced pores contribute additional membrane strain to the lipid vesicle, which eventually leads to membrane lysis after a critical density of pores is reached. Similar trends in the critical P:L ratio were obtained with lipid vesicles possessing biologically relevant membrane compositions. The specifics of the kinetics observed have been explained by using a generic kinetic model, and the model predictions are based primarily on exponents that were earlier measured in independent experiments. Looking forward, there is significant opportunity to further explore how AH peptide exerts virucidal activity against highly curved virion envelopes, particularly in the context of strain-induced membrane lysis arising from pore formation.

ASSOCIATED CONTENT

Supporting Information

The Supporting Information is available free of charge on the ACS Publications website at DOI: 10.1021/jacs.5b12491.

Supplementary methods and supporting QCM-D experimental analysis and kinetic model analysis. (PDF)

AUTHOR INFORMATION

Corresponding Author

*njcho@ntu.edu.sg

Notes

The authors declare no competing financial interest.

ACKNOWLEDGMENTS

We acknowledge the National Research Foundation (NRF-NRFF2011-01) and the National Medical Research Council (NMRC/CBRG/0005/2012) for financial support. V.P.Zh. is a recipient of the Tan Chin Tuan Exchange Fellowship at Nanyang Technological University.

REFERENCES

(1) Marston, H. D.; Folkers, G. K.; Morens, D. M.; Fauci, A. S. *Sci. Transl. Med.* **2014**, *6*, 253ps10.
(2) Miller, S.; Krijnse-Locker, J. *Nat. Rev. Microbiol.* **2008**, *6*, 363.
(3) De Clercq, E. *Nat. Rev. Drug Discovery* **2002**, *1*, 13.
(4) Mercer, J.; Schelhaas, M.; Helenius, A. *Annu. Rev. Biochem.* **2010**, *79*, 803.
(5) Wolf, M. C.; Freiberg, A. N.; Zhang, T.; Akyol-Ataman, Z.; Grock, A.; Hong, P. W.; Li, J.; Watson, N. F.; Fang, A. Q.; Aguilar, H. C. *Proc. Natl. Acad. Sci. U. S. A.* **2010**, *107*, 3157.
(6) Vincent, M. R. S.; Colpitts, C. C.; Ustinov, A. V.; Muqadas, M.; Joyce, M. A.; Barsby, N. L.; Epand, R. F.; Epand, R. M.; Khramyshev, S. A.; Valueva, O. A. *Proc. Natl. Acad. Sci. U. S. A.* **2010**, *107*, 17339.
(7) Vigant, F.; Lee, J.; Hollmann, A.; Tanner, L. B.; Ataman, Z. A.; Yun, T.; Shui, G.; Aguilar, H. C.; Zhang, D.; Meriwether, D. *PLoS Pathog.* **2013**, *9*, e1003297.
(8) Vigant, F.; Hollmann, A.; Lee, J.; Santos, N. C.; Jung, M. E.; Lee, B. *J. Virol.* **2014**, *88*, 1849.
(9) Cheng, G.; Montero, A.; Gastaminza, P.; Whitten-Bauer, C.; Wieland, S. F.; Isogawa, M.; Fredericksen, B.; Selvarajah, S.; Gallay, P. A.; Ghadiri, M. R. *Proc. Natl. Acad. Sci. U. S. A.* **2008**, *105*, 3088.
(10) Cho, N.-J.; Dvory-Sobol, H.; Xiong, A.; Cho, S.-J.; Frank, C. W.; Glenn, J. S. *ACS Chem. Biol.* **2009**, *4*, 1061.
(11) Tabaei, S. R.; Rabe, M.; Zhdanov, V. P.; Cho, N. J.; Höök, F. *Nano Lett.* **2012**, *12*, 5719.
(12) Jackman, J. A.; Saravanan, R.; Zhang, Y.; Tabaei, S. R.; Cho, N.-J. *Small* **2015**, *11*, 2372.
(13) Edelhoch, H. *Biochemistry* **1967**, *6*, 1948.
(14) Wimley, W. C. *ACS Chem. Biol.* **2010**, *5*, 905.
(15) Melo, M. N.; Ferre, R.; Castanho, M. A. *Nat. Rev. Microbiol.* **2009**, *7*, 245.
(16) Papo, N.; Shai, Y. *Peptides* **2003**, *24*, 1693.
(17) Melo, M. N.; Castanho, M. A. *Front. Immunol.* **2012**, DOI: 10.3389/fimmu.2012.00236.
(18) Wimley, W. C.; Hristova, K. *J. Membr. Biol.* **2011**, *239*, 27.
(19) Rathinakumar, R.; Wimley, W. C. *J. Am. Chem. Soc.* **2008**, *130*, 9849.
(20) Cho, N.-J.; Cho, S.-J.; Cheong, K. H.; Glenn, J. S.; Frank, C. W. *J. Am. Chem. Soc.* **2007**, *129*, 10050.
(21) Cho, N.-J.; Frank, C. W.; Kasemo, B.; Höök, F. *Nat. Protoc.* **2010**, *5*, 1096.
(22) Richter, R. P.; Brisson, A. R. *Biophys. J.* **2005**, *88*, 3422.
(23) Cho, N.-J.; Wang, G.; Edvardsson, M.; Glenn, J. S.; Höök, F.; Frank, C. W. *Anal. Chem.* **2009**, *81*, 4752.
(24) Jackman, J. A.; Zan, G. H.; Zhdanov, V. P.; Cho, N.-J. *J. Phys. Chem. B* **2013**, *117*, 16117.

DOI: 10.1021/jacs.5b12491
J. Am. Chem. Soc. 2016, 138, 1406−1413

(25) Gidalevitz, D.; Ishitsuka, Y.; Muresan, A. S.; Konovalov, O.; Waring, A. J.; Lehrer, R. I.; Lee, K. Y. C. *Proc. Natl. Acad. Sci. U. S. A.* **2003**, *100*, 6302.
(26) Keller, C.; Glasmästar, K.; Zhdanov, V.; Kasemo, B. *Phys. Rev. Lett.* **2000**, *84*, 5443.
(27) Palomares-Jerez, M. F.; Guillén, J.; Villalaín, J. *Biochim. Biophys. Acta, Biomembr.* **2010**, *1798*, 1212.
(28) Zhdanov, V. P.; Höök, F. *Phys. Rev. E: Stat., Nonlinear, Soft Matter Phys.* **2013**, *87*, 042718.
(29) Brügger, B.; Glass, B.; Haberkant, P.; Leibrecht, I.; Wieland, F. T.; Kräusslich, H.-G. *Proc. Natl. Acad. Sci. U. S. A.* **2006**, *103*, 2641.
(30) Róg, T.; Vattulainen, I. *Chem. Phys. Lipids* **2014**, *184*, 82.
(31) Goh, H. Z.; Jackman, J. A.; Cho, N.-J. *J. Phys. Chem. B* **2014**, *118*, 3616.
(32) Taheri-Araghi, S.; Ha, B.-Y. *Phys. Rev. Lett.* **2007**, *98*, 168101.
(33) Huang, H. W.; Chen, F.-Y.; Lee, M.-T. *Phys. Rev. Lett.* **2004**, *92*, 198304.
(34) Huang, H. W. *Biochim. Biophys. Acta, Biomembr.* **2006**, *1758*, 1292.
(35) Chen, F.-Y.; Lee, M.-T.; Huang, H. W. *Biophys. J.* **2003**, *84*, 3751.
(36) Fadda, G.; Lairez, D.; Guennouni, Z.; Koutsioubas, A. *Phys. Rev. Lett.* **2013**, *111*, 028102.
(37) Lee, M.-T.; Sun, T.-L.; Hung, W.-C.; Huang, H. W. *Proc. Natl. Acad. Sci. U. S. A.* **2013**, *110*, 14243.
(38) Lee, J.-H.; Choi, S.-M.; Doe, C.; Faraone, A.; Pincus, P. A.; Kline, S. R. *Phys. Rev. Lett.* **2010**, *105*, 038101.
(39) Cho, N.-J.; Cho, S.-J.; Hardesty, J. O.; Glenn, J. S.; Frank, C. W. *Langmuir* **2007**, *23*, 10855.
(40) Wang, J.; Liu, K.-W.; Biswal, S. L. *Anal. Chem.* **2014**, *86*, 10084.

DOI: 10.1021/jacs.5b12491
J. Am. Chem. Soc. 2016, 138, 1406−1413